DOI: 10.1002/ejoc.201000774

Theoretical Investigations towards the Staudinger Reaction Catalyzed by N-Heterocyclic Carbene: Mechanism and Stereoselectivity

Ke Tang,[a] Jinhu Wang,[a] Xueli Cheng,[a] Qianqian Hou,[a] and Yongjun Liu*[a]

Keywords: Heterocycles / Carbenes / Reaction mechanisms / Stereoselectivity / Density functional calculations

N-Heterocyclic carbenes (NHCs) have experimentally proved to be powerful catalysts for the Staudinger reaction ([2+2] cycloaddition of a ketene with an imine) but without giving a clear catalytic mechanism. According to different experimental results, the "ketene-first" and the "imine-first" mechanisms, arguing which reactant should be initially activated by the NHC catalyst, have been proposed. Our theoretical investigation by employing density functional theory (DFT) reveals that the reaction mechanism of the NHC-catalyzed Staudinger reaction is exclusively the "ketene-first" mechanism, but the competitive reactions of NHC catalysts with ketenes or imines will lead to different experimental observations. On the basis of this conclusion, we found that the NHC-catalyzed Staudinger reaction would exhibit different stereoselectivities by appropriate choice of the nitrogen substituent of the imines. Furthermore, these results are supposed to be applicable for other nucleophile-catalyzed Staudinger reactions.

Introduction

The biological activity of β-lactams as antibacterial agents[1] and further utility as pharmaceutical intermediates[2] have been prompting persistent synthetic activities of the β-lactam skeleton for about one century. Although various methods have been developed in succession,[3] the Staudinger reaction,[4] the first one reported in 1907 and characterized by [2+2] cycloaddition of a ketene with an imine, remains the most widely used method for its versatility and efficiency.[5] Generally, the outcome of this reaction is limited to achiral or racemic products, and chiral auxiliaries are usually required to overcome this disadvantage.[6] Not long ago, a more general methodology based on asymmetric catalysis was successfully applied to the Staudinger reaction by Lectka et al. to furnish β-lactams with high enantioselectivity in the presence of a quinine-derived catalyst.[7] Central conception of this methodology lies in umpolung catalysis, which makes the reaction start with reversed polarity, namely, the two reactants switch their roles that they play in the classical Staudinger reaction.[8] Inspired by this pioneering strategy, Fu et al. broadened the scope of this reaction to include unsymmetrical disubstituted ketenes by using a series of 4-(pyrrolidino)pyridine (PPY) derivatives as catalysts; therefore, optically active trisubstituted β-lactams were generated with not only good enantioselectivity but also diastereoselectivity.[9]

Encouraged by the first successful isolation of a stable carbene in 1991,[10] the full application of N-heterocyclic carbenes (NHCs) as powerful catalysts in organic synthesis has been demonstrated impressively.[11] Recently, their efficient catalysis of Staudinger reactions was also proved able to guarantee equivalent yields with a wider range of reactants.[12] However, in contrast to the successful practical application, synchronous mechanistic investigations are quite insufficient and the catalytic mechanism remains unclear. Up to date, two possible mechanisms have been proposed, arguing which reactant should be initially activated by the NHC catalyst (Scheme 1).[12a] As for the denoted "ketene-first" mechanism A, the nucleophilic catalyst initially attacks the ketene to generate the NHC–ketene zwitterionic intermediate $IN1_A$, which is followed by a Mannich-like reaction between this enolate and the imine to form $IN2_A$. Finally, the cyclization of $IN2_A$ to the product liberates the catalyst and closes the reaction pathway. Alternatively, in the "imine-first" mechanism B these two reactants interchange their order: the imine instead of the ketene is activated by the catalyst, leading to the formation of $IN1_B$. Then, the highly nucleophilic NHC–imine zwitterion $IN1_B$ attacks the ketene to form enolate $IN2_B$. Subsequent [4-*exo*-*tet*] cyclization of $IN2_B$ regenerates the catalyst and furnishes the final product.

Experimental results from different groups do not converge at an agreement but even contradict each other to some extent. The experiment carried out by Smith et al. showed that the addition of diphenylketene to the catalyst

[a] Key Laboratory of Colloid and Interface Chemistry, Ministry of Education, School of Chemistry and Chemical Engineering, Shandong University,
Jinan, 250100, P. R. China
E-mail: yongjunliu_1@sdu.edu.cn

Supporting information for this article is available on the WWW under http://dx.doi.org/10.1002/ejoc.201000774.

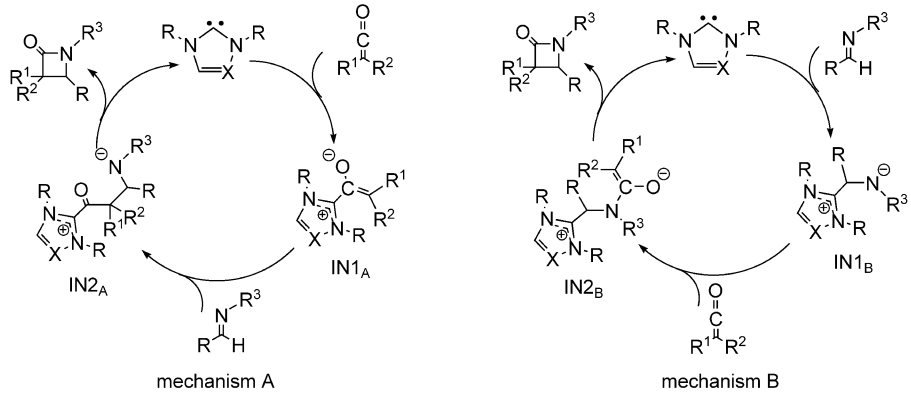

Scheme 1. Two proposed mechanisms for the NHC-catalyzed Staudinger reaction: the "ketene-first" mechanism A and the "imine-first" mechanism B.[12a]

(triazolinylidene) followed by *N*-tosyl (Ts) imine gives excellent conversion to β-lactam, whereas the reverse addition order of reactants gives no conversion [Equation (1)],[12b] obviously supporting the "ketene-first" mechanism A. However, when *N*,*N*′-bis(2,6-diisopropylphenyl)imidazol-2-ylidene was used, Ye et al. identified the NHC–imine zwitterion ($IN1_B$) rather than the NHC–ketene zwitterion ($IN1_A$); after being isolated, the zwitterion could further react with phenylethylketene to give β-lactam [Equation (2)],[12a] which implies the possibility of "imine-first" mechanism B. More evidence in support of mechanism B is from the aforementioned PPY derivative catalyzed system, in which the adduct of the catalyst with a more electrophilic *N*-triflyl (Tf) imine was crystallized.[9a] However, it is interesting to find that when *N*-Tf imine was replaced by *N*-Ts imine, the interaction between the catalyst and the imine cannot be detected by ^{1}H NMR spectroscopy, and accompanied with the different behaviors of the two *N*-Ts/Tf imines are the divergent *cis*/*trans* stereoselective preferences of the final products (Scheme 2). These unexpected results naturally led the authors to suggest that both mechanisms are feasible but are dependent on the different N-substituents of the imine.

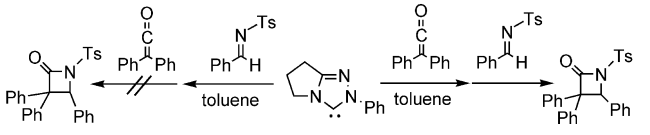

(1)

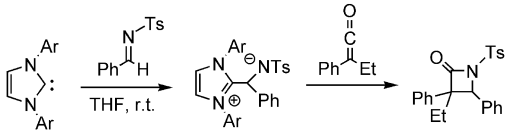

(2)

Numerous investigations have been devoted to the classical Staudinger reaction during the past decades, disclosing that the mechanism of the Staudinger reaction is much more complicated than its simple appearance.[13] Apparently, new challenges to the mechanical exploration of the Staudinger reaction have been posed by the catalytic reactions and little attention has been paid to this point.[8,14] Herein, a theoretical investigation on the NHC-catalyzed Staudinger reaction has been carried out by using density functional theory (DFT) to get an in-depth understanding of the catalyzed Staudinger reaction mechanism. The potential relationship between the electrophilicity of imines and reaction stereoselectivity, which has not been systematically studied before, is also addressed here.

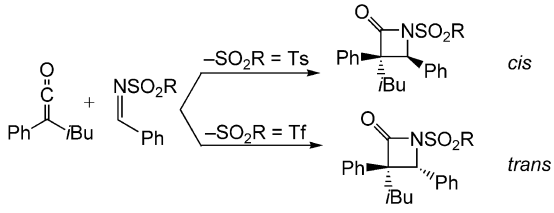

Scheme 2. Different *cis*/*trans* stereoselective preferences for Staudinger reactions reported by Fu et al.[9a]

Models and Computational Details

For simplicity, 1,3-dimethyltriazolylidene was used as a template for the NHC catalyst in our calculations.[15] The reactants, disubstituted phenylmethylketene and *N*-Ts imine, come from the reported experiment.[12a] To make sure whether the electrophilicity of the imine is one determinant of the Staudinger reaction mechanism, *N*-Tf imine was borrowed from the aforementioned PPY derivative catalyzed system.[9a] Here, only the (*E*)-stereoisomer of the imines was considered because most imines employed in the Staudinger reaction have been experimentally determined to be exclusively of *E* configuration.[16] Full geometry optimizations and harmonic vibrational frequencies were calculated at the B3LYP[17] level of theory with the 6-31G(d) basis set in the gas phase, and solvent effects were taken into account for single-point calculations by using a CPCM polarizable conductor calculation model.[18,19] The solvent was set to THF, which was used in experiments. The corresponding energies

were corrected with zero-point vibrational energy by using unscaled frequencies.[20] The structure of the transition state with exactly one imaginary frequency was further validated by intrinsic reaction coordinate (IRC)[21] analysis.

Results and Discussion

Reaction Mechanism

The stereochemical processes of the two mechanisms are considered as follows: for the "ketene-first" mechanism A, the *exo* or *endo* attack of the NHC on the ketene gives $IN1_A$ of *Z* and *E* configurations, respectively. Each one can take the *Re* or *Si* face to react with the imine from the *Re* or *Si* side to generate $IN2_A$. Thus, eight possible reaction patterns exist and four of them lead to *trans* products and the other four to *cis* products (Table 1). Considering the steric effect, only the *exo* attack occurring at the less-hindered side of the ketene was taken into account (Scheme 3A). Similarly, for the "imine-first" mechanism B, the NHC may attack the imine from *the Re* or *Si* face to give intermediate $IN1_B$ (two enantiomers of *S* and *R* configurations). The enantiomers then react with the ketene through *exo* and *endo* attack to generate (*Z*)- and (*E*)-$IN2_B$, respectively. Overall, four possible reaction patterns would be obtained, as shown in Table 2. As the enantiomers have identical properties, only the case of (*R*)-$IN1_B$ was considered in our calculations (Scheme 3B). Calculated relative free energies (ΔG_{sol}) of different reaction patterns are listed in Tables 3 and 4 for mechanisms A and B, respectively, and the most energetically favored ones thereinto are depicted in Figure 1 with the *N*-Tf imine system in bracket.

Table 1. Eight possible reaction patterns for mechanism A.

Reaction pattern	Configuration IN1A	IN1A	Reacting face (*E*)-imine	Product
$Z_{Si–Si}$	*Z*	*Si*	*Si*	*trans*
$Z_{Si–Re}$	*Z*	*Si*	*Re*	*cis*
$Z_{Re–Re}$	*Z*	*Re*	*Re*	*trans*
$Z_{Re–Si}$	*Z*	*Re*	*Si*	*cis*
$E_{Si–Si}$	*E*	*Si*	*Si*	*cis*
$E_{Si–Re}$	*E*	*Si*	*Re*	*trans*
$E_{Re–Re}$	*E*	*Re*	*Re*	*cis*
$E_{Re–Si}$	*E*	*Re*	*Si*	*trans*

Table 2. Four possible reaction patterns for mechanism B.

Reaction pattern	Reacting face (*E*)-imine	Configuration $IN1_B$	$IN2_B$	Product
R_{exo}	*Si*	*R*	*Z*	*cis*
R_{endo}	*Si*	*R*	*E*	*trans*
S_{exo}	*Re*	*S*	*Z*	*cis*
S_{endo}	*Re*	*S*	*E*	*trans*

As shown in Figure 1, for the *N*-Ts system, the energy difference between the rate-determining steps of pathway A ($IN2_A \rightarrow 3_A$) and pathway B ($IN2_B \rightarrow 3_B$) is as much as 30.5 kcal/mol, indicating that the "ketene-first" pathway A is much more favorable than the "imine-first" pathway B. Besides, the overall energy barrier of pathway B reaches 34.9 kcal/mol. Such a high energy barrier suggests that

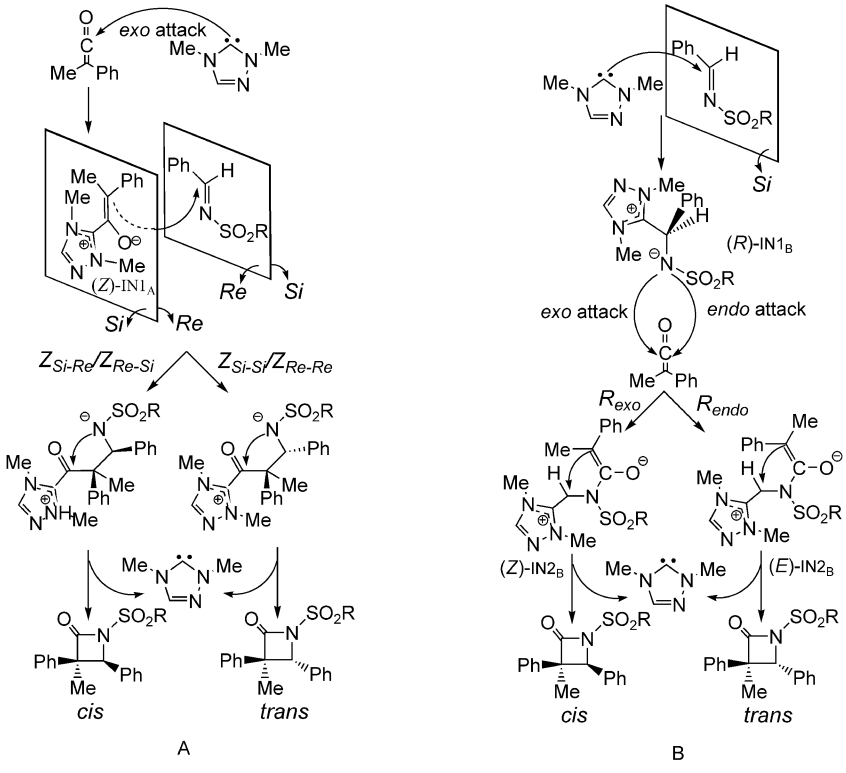

Scheme 3. Illustration of the considered stereochemical processes of mechanisms A and B.

Table 3. Calculated free energies in solvent THF ($\Delta G_{sol\ =\ THF}$) for mechanism A at the B3LYP/6-31G(d) level (in kcal/mol).

	0_A	$TS1_A$	$IN1_A$	$TS2_A$	$IN2_A$	$TS3_A$	3_A
							N-Ts system
$Z_{Si–Si}$	0	1.3	–22.8	4.7	–5.5	3.4	–12.0
$Z_{Si–Re}$	0	1.3	–22.8	6.1	1.1	7.2	–11.0
$Z_{Re–Re}$	0	1.3	–22.8	6.2	–4.4	2.8	–12.0
$Z_{Re–Si}$	0	1.3	–22.8	1.6	–1.0	4.4	–11.0
							N-Tf system
$Z_{Si–Si}$	0	1.3	–22.8	–5.8	–14.5	–0.2	–11.2
$Z_{Si–Re}$	0	1.3	–22.8	–8.0	–13.4	3.0	–10.3
$Z_{Re–Re}$	0	1.3	–22.8	–1.9	–10.7	–0.8	–11.2
$Z_{Re–Si}$	0	1.3	–22.8	–7.7	–13.1	1.3	–10.3

Table 4. Calculated free energies in solvent THF ($\Delta G_{sol\ =\ THF}$) for mechanism B at the B3LYP/6-31G(d) level (in kcal/mol).

	0_B	$TS1_B$	$IN1_B$	$TS2_B$	$IN2_B$	$TS3_B$	3_B
							N-Ts system
R_{exo}	0	5.8	–10.1	0.9	–5.8	35.3	–13.3
R_{endo}	0	5.8	–10.1	7.8	–2.2	34.9	–14.3
							N-Tf system
R_{exo}	0	2.9	–19.6	–9.8	–12.9	36.4	–11.5
R_{endo}	0	2.9	–19.6	–7.9	–11.3	35.2	–12.5

mechanism B is actually unfeasible, considering that the experiments are usually carried out at room temperature or below. Furthermore, as can be seen from Table 4, the energy barrier difference between the two reaction patterns of pathway B is only 0.4 kcal/mol. This result implies that the distinct stereoselective preference displayed in the experiments[12] would not be achieved provided that the catalytic Staudinger reaction proceeds through pathway B. Of particular note is the finding that mechanism A basically belongs to umpolung catalysis, which has been successfully introduced into the catalytic asymmetric Staudinger reactions by Lectka et al.[8] As shown in pathway A, the imine acts as an electrophile and the ketene as a nucleophile, which is opposite to the roles they play in the classical Staudinger pathway (in which the imine acts as a nucleophile toward the ketene). As for pathway B, the roles of the reactants remain the same as that in the classical Staudinger reaction. Combination of these factors suggests that the "ketene-first" mechanism A is much more feasible than the "imine-first" mechanism B for the NHC-catalyzed Staudinger reaction.

Fu et al. proposed that the catalytic mechanism of the Staudinger reaction might switch from A to B when *N*-Tf imine takes the place of *N*-Ts imine in their PPY derivative catalyzed system.[9a] However, our calculations find that this mechanistic change is unlikely to happen. As can be seen from Figure 1, when the *N*-Ts imine is replaced by *N*-Tf imine, the energy barrier of pathway B increases only by 0.3 kcal/mol, and meanwhile that of pathway A reduces by 5.2 kcal/mol. That is to say, the replacement of *N*-Ts by *N*-Tf in the imine makes pathway A more energetically preferential. It can be explained by the fact that, acting as electrophiles in pathway A, *N*-Tf imine with stronger electrophilicity is more active than *N*-Ts imine. The result further supports our conclusion that mechanism A is more feasible for NHC-catalyzed Staudinger reactions.

From Figure 1 we also note that the relative free energy of $TS1_B$ is only 5.8 kcal/mol, meaning the reaction of the catalyst with *N*-Ts imine is also facile, which has been experimentally confirmed by the isolation of the NHC–imine $IN1_B$.[12a] Further study indicates that the $IN1_B$ could react with ketene to generate the β-lactam as well, as if the reaction proceeds through the "imine-first" pathway B. The explanation from the authors for this point is that $IN1_B$ may decompose in situ into the initial reactants and then form the β-lactam through pathway A.[22] Our calculations may well explain this hypotheses. The difference in energy barriers of the formation and decomposition of $IN1_B$ is calcu-

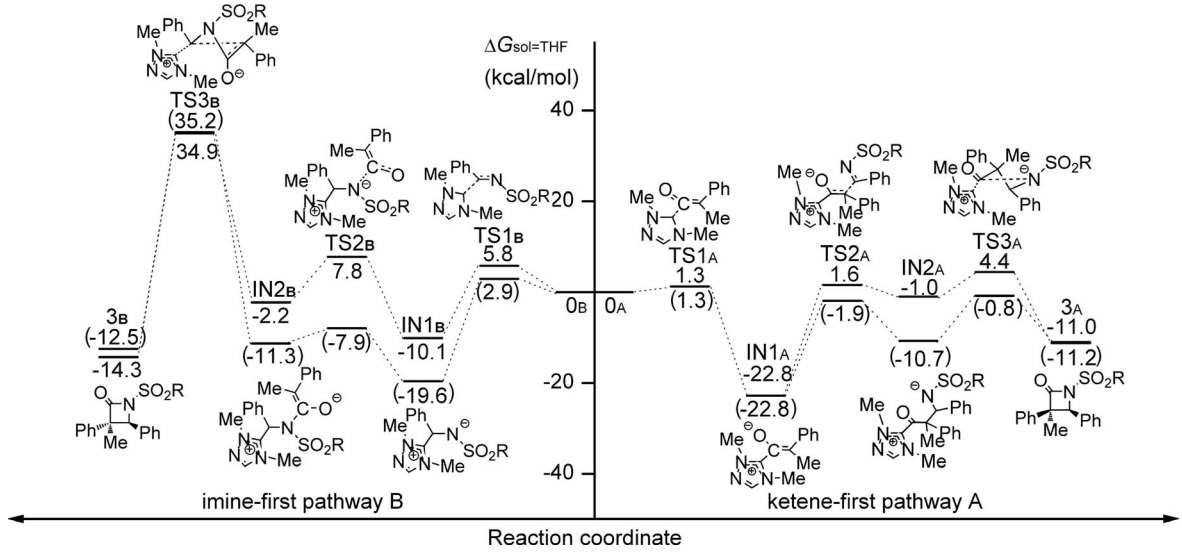

Figure 1. Calculated free-energy profiles of the most energetically favored reaction patterns for systems of *N*-Ts imine and *N*-Tf imine (in bracket) at the CPCM-B3LYP/6-31G(d) level.

lated to be only –10.1 kcal/mol, so the break up of $IN1_B$ is easy. Meanwhile, we also found that the energy barrier difference between the formation of $IN1_B$ and its reverse extends to –19.6 kcal/mol for the more electrophilic *N*-Tf imine system. This implies that the formation of $IN1_B$ might not always be a reversible process if the electrophilicity of the imine increases to some extent. The reaction would stop at the stage of forming relatively stable $IN1_B$, that is, the catalytic activity of the NHC is inhibited through the formation of stable catalyst–imine adducts and the expected product could not be obtained. This point is believed to be a reasonable explanation for the experiment carried out by Smith et al. that the addition of the imine to the catalyst followed by the ketene gives no conversion to the β-lactam [Equation (1)].[12b] It is noteworthy that the activity inhibition of the NHCs arising from the reaction with electrophilic imines has been confirmed by experiments.[23]

On the basis of the overall considerations of the above discussions, we conclude that the mechanism of the NHC-catalyzed Staudinger reaction is exclusively the "ketene-first" mechanism A, but a competition between the reactions of NHC catalysts with ketenes (K) or imines (I) will lead to different experimental observations. A general prediction about the experimental results is illustrated in Figure 2. As displayed, when the reaction rate constant of the catalyst coupling with the ketene (k_1) is larger than that with the imine (k_{2+}), the reaction proceeds directly through pathway A to generate the β-lactam without the observation of $IN1_B$. On the contrary, if k_1 is smaller than k_{2+}, the catalyst prefers to react with the imine rather than the ketene to form $IN1_B$, which may decompose into the initial reactants ($k_{2+} \approx k_{2-}$) or not ($k_{2+} >> k_{2-}$). For the former case, the reaction still follows pathway A to give the final product, but the latter case only gives the stable $IN1_B$.

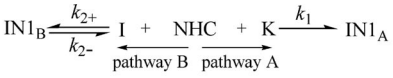

		$IN1_B$	β-lactam
$k_1 > k_{2+}$		×	v
$k_1 < k_{2+}$	$k_{2+} \approx k_{2-}$	v	v
	$k_{2+} >> k_{2-}$	v	×

Figure 2. General kinetic prediction of possible experimental results.

Reaction Stereoselectivity

NHCs are regarded to be typical nucleophilic catalysts in Staudinger reactions, so the results derived from the NHC-catalyzed system are rationally believed to be applicable in the other nucleophile-catalyzed Staudinger reactions. It occurs to us that the divergent stereoselective preferences of the nucleophile-catalyzed Staudinger reactions would not originate from different mechanisms but from other stereochemical factors. Therefore, a series of *N*-sulfonyl (*N*-SO_2R) imines bearing different substituents [R = CH_3-, C_6H_5-, 4-$(CF_3)C_6H_4$-, and 4-$(NO_2)C_6H_4$-] was supplemented to get a systematic view. As depicted in Scheme 3, the stereoselectivity is determined by the step $IN1_A \rightarrow IN2_A$ for pathway A. So the discussion of stereochemical control focuses only on this step. The calculated relative free energies of $TS2_A$ are displayed in Figure 3. To differentiate the electrophilicity of imines, the calculated Mulliken charge distributions of the sulfonyl group of imine monomers are denoted by abscissa.

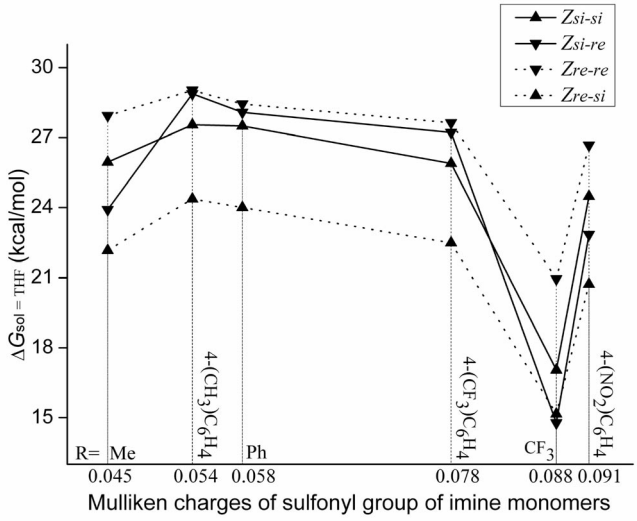

Figure 3. Calculated relative free energies of TS_{2A} in solvent THF ($\Delta G_{sol\ =\ THF}$) for different reaction patterns at the B3LYP/6-31G(d) level.

As shown in Figure 3, for reaction patterns Z_{Re-Re} and Z_{Re-Si} (denoted by symbols with dotted lines) in which $IN1_A$ takes the *Si* face in the reaction, the free energies (ΔG_{sol}) of $TS2_A(Z_{Re-Si})$ are always lower than those of $TS2_A(Z_{Re-Re})$ for all six systems, meaning an exclusive *cis* stereoselectivity independent of the choice of imines. Interestingly, for the other case where $IN1_A$ assumes the *Re* face to react with imines (symbols with solid lines), the reaction stereoselectivity diverges according to the bulk size of the N-substituents of the imines. For systems of imines with small N-substituents (R = CH_3- and CF_3-), the values of ΔG_{sol} of $TS2_A(Z_{Si-Re})$ are lower than that of $TS2_A(Z_{Si-Si})$, which leads to *trans* stereopreference, whereas for other bulky *N*-substituted systems, reaction pattern Z_{Si-Si} is more preferential than pattern Z_{Si-Re} with the *cis* stereoselectivity favored. An exception is the system with the most electrophilic imine [R = 4-$(NO_2)C_6H_4$-]. Unlike other bulky *N*-substituted systems with *cis* stereoselectivity, it is *trans* selective.

To get a visual understanding of the origins of the above results, the optimized structures of $TS2_A$ for the *N*-Ts imines along with electrostatic potential (ESP)-mapped electron density surfaces are illustrated in Figure 4. As displayed, two major factors are regarded to be responsible for the stereoselectivities. One is the static repulsion between the *N*-sulfonyl group and carbonyl group, and the other is the steric exclusion resulting from the bulky *N*-sulfonyl

group. As can be seen, in the reaction patterns $Z_{Re–Si}$ and $Z_{Re–Re}$, the two effects cooperate with each other making both the two interactions strong in $TS2_A(Z_{Re–Re})$ (denoted as S,S in Figure 4) and weak in $TS2_A(Z_{Re–Si})$ (denoted as W, W) no matter the nature of the imine. That is why we cannot see the intersection of the two dotted lines in Figure 4. However, for other reaction patterns, the two effects behave in a negative manner leading to a strong static repulsion but a weak steric exclusion in $TS2_A(Z_{Si–Si})$ (denoted as S, W), and a weak static repulsion and strong steric exclusion in $TS2_A(Z_{Si–Re})$ (denoted as W, S). For imines with small N-substituents, the contribution from static repulsion overwhelms that of steric exclusion, and therefore, the reaction pattern $Z_{Si–Re}$ is preferred. In contrast, if the imine bears a bulky N-substituent, the steric exclusion will overcome the static repulsion and the reaction pattern $Z_{Si–Si}$ becomes favored. The special case of 4-$(NO_2)C_6H_4$ implies that the stereoselectivity may be predominantly controlled by static effects when the electrophilicity of the imines increases to some extent.

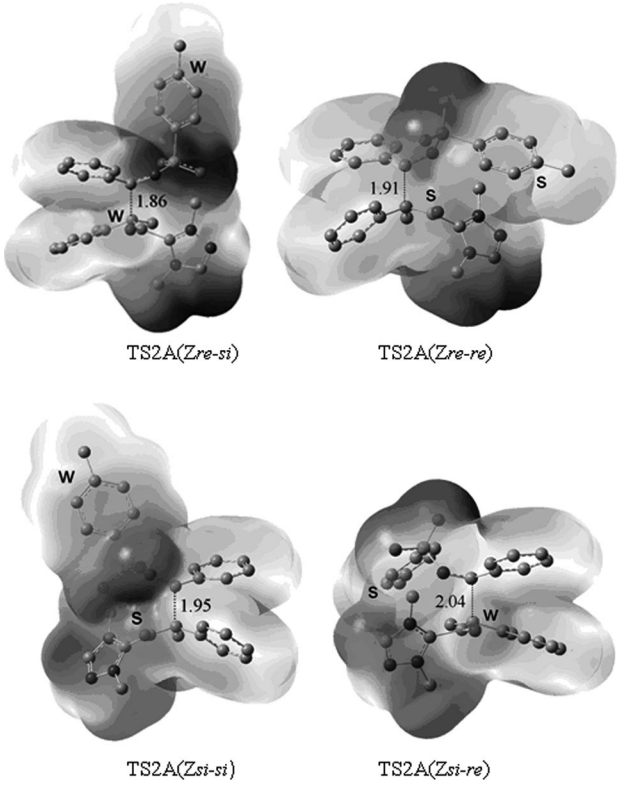

Figure 4. Optimized structures of $TS2_A$ with key parameters and electrostatic potential (ESP)-mapped electron density surfaces for the *N*-Ts imine system at the B3LYP/6-31G(d) level. Distances are given in Å. S (strong) and W (weak) denote the relative intensity of the static and steric effects. All hydrogen atoms are omitted for clarity.

The above discussions reveal that the catalytic Staudinger reaction will exhibit divergent *trans*/*cis* preferences through the appropriate choice of the *N*-substituents of the imines on condition that $IN1_A$ assumes one certain face in the reactions [Equations (1) and (2)]. The point that the exclusive reaction on one face of the "NHC–reactant" intermediate would be accomplished through proper steric and/or electronic modification of the substituents of the NHCs has been experimentally[24] and computationally[15a,25] proven.

Conclusions

The theoretical calculations on the two proposed reaction mechanisms demonstrate that the "ketene-first" mechanism A is much more feasible than the "imine-first" mechanism B in the NHC-catalyzed Staudinger reaction. The change of electrophilicity in the imines does not alter the reaction mechanism but leads to different experimental observations. On the basis of this conclusion, we found that the catalytic Staudinger reaction will exhibit divergent stereoselectivities and follows the unique mechanism A. Further study with full consideration of different substituents on the NHC catalysts is underway with the hope of getting a thorough understanding of the catalytic Staudinger reaction.

Supporting Information (see footnote on the first page of this article): Absolute energies of the species involved in mechanisms A and B and those of $TS2_A$ for systems of *N*-sulfonyl imines [R = CH_3-, 4-(CH_3)-C_6H_4-, C_6H_5-, 4-$(CF_3)C_6H_4$-, -CF_3, and 4-$(NO_2)C_6H_4$-] as well as the corresponding atomic coordinates.

Acknowledgments

This work was supported by the Independent Innovation Foundation of Shandong University (2009JC018) and Natural Science Foundation of China (20873075).

[1] a) K. B. Holten, E. M. Onusko, *Am. Fam. Physician* **2000**, *62*, 611–620; b) B. Kasten, R. Reski, *J. Plant Physiol.* **1997**, *150*, 137–140; c) O. A. Mascaretti (Ed.), *The β-Lactamases: A Major Cause of Resistance of β-Lactam Antibiotics and β-Lactamase Inhibitors*, Bentham, Hilversum, Netherlands, **1999**.

[2] a) B. Alcaide, P. Almendros, *Curr. Med. Chem.* **2004**, *11*, 1921–1949; b) D. I. Kingston, *Chem. Commun.* **2001**, *10*, 867–880; c) G. S. Singh, *Tetrahedron* **2003**, *59*, 7631–7649; d) C. Palomo, J. M. Aizpurua, I. Ganboa, M. Oiarbide, *Synlett* **2001**, *12*, 1813–1826.

[3] For other notable methods such as the Gilman–Speeter reaction, photoinduced rearrangements, and radical cyclizations, see: a) H. Gilman, M. Speeter, *J. Am. Chem. Soc.* **1943**, *65*, 2255–2256; b) S. Kobayashi, T. Iimori, T. Izawa, M. Ohno, *J. Am. Chem. Soc.* **1981**, *103*, 2406–2047; c) H. Ishibashi, C. Kameoka, K. Kodama, M. Ikeda, *Tetrahedron* **1996**, *52*, 489–502; d) H. Fujieda, M. Kanai, T. Kambara, A. Iida, K. A. Tomioka, *J. Am. Chem. Soc.* **1997**, *119*, 2060–2061; e) F. Toda, H. Miyamoto, M. Inoue, S. Yasaka, I. Matijasic, *J. Org. Chem.* **2000**, *65*, 2728–2732.

[4] H. Staudinger, *Justus Liebigs Ann. Chem.* **1907**, *356*, 51–123.

[5] For reviews on the Staudinger reaction, see: a) D. H. Paull, A. Weatherwax, T. Lectka, *Tetrahedron* **2009**, *65*, 6771–6803; b) T. T. Tidwell, *Angew. Chem. Int. Ed.* **2008**, *47*, 1016–1020; c) C. Palomo, J. M. Aizpurua, I. Ganboa, M. Oiarbide, *Curr. Med. Chem.* **2004**, *11*, 1837–1872; d) C. Palomo, J. M. Aizpurua, I. Ganboa, M. Oiarbide, *Eur. J. Org. Chem.* **1999**, *12*, 3223–3235; e) R. G. D. Cooper, B. W. Daugherty, D. B. Boyd, *Pure Appl. Chem.* **1987**, *59*, 485–492.

[6] a) D. A. Evans, E. B. Sjogren, *Tetrahedron Lett.* **1985**, *26*, 3783–3786; b) A. K. Bose, M. S. Manhas, J. M. van der Veen, S. S. Bari, D. R. Wagle, *Tetrahedron* **1992**, *48*, 4831–4844.

[7] A. E. Taggi, A. M. Hafez, H. Wack, B. Young, W. J. Drury III, T. Lectka, *J. Am. Chem. Soc.* **2000**, *122*, 7831–7832.
[8] S. France, A. Weatherwax, A. E. Taggi, T. Lectka, *Acc. Chem. Res.* **2004**, *37*, 592–600.
[9] a) E. C. Lee, B. L. Hodous, E. Bergin, C. Shih, G. C. Fu, *J. Am. Chem. Soc.* **2005**, *127*, 11586–11587; b) B. L. Hodous, G. C. Fu, *J. Am. Chem. Soc.* **2002**, *124*, 1578–1579.
[10] A. J. Arduengo III, R. L. Harlow, M. Kline, *J. Am. Chem. Soc.* **1991**, *113*, 361–363.
[11] D. Enders, O. Niemeier, H. Alexander, *Chem. Rev.* **2007**, *107*, 5606–5655.
[12] a) Y. R. Zhang, L. He, X. Wu, P. L. Shao, S. Ye, *Org. Lett.* **2008**, *10*, 277–280; b) N. Duguet, C. D. Campbell, A. M. Z. Slawin, A. D. Smith, *Org. Biomol. Chem.* **2008**, *6*, 1108–1113.
[13] For recent reviews on mechanistic investigations of the Staudinger reaction, see: a) F. P. Cossío, A. Arrieta, M. A. Sierra, *Acc. Chem. Res.* **2008**, *41*, 925–936; b) N. Y. Fu, T. T. Tidwell, *Tetrahedron* **2008**, *64*, 10465–10496; c) Y. Liang, L. Jiao, S. W. Zhang, Z. X. Yu, J. X. Xu, *J. Am. Chem. Soc.* **2009**, *131*, 1542–1549; d) L. Jiao, Y. Liang, J. X. Xu, *J. Am. Chem. Soc.* **2006**, *128*, 6060–6069; e) A. Venturini, J. González, *J. Org. Chem.* **2002**, *67*, 9089–9092; f) A. Arrieta, B. Lecea, F. P. Cossío, *J. Org. Chem.* **1998**, *63*, 5869–5876.
[14] A. E. Taggi, A. M. Hafez, T. Dudding, T. Lectka, *Tetrahedron* **2002**, *58*, 8351–8356.
[15] For other examples of simplified templates as NHC catalysts, see: a) K. J. Hawkes, B. F. Yates, *Eur. J. Org. Chem.* **2008**, *33*, 5563–5570; b) B. Goldfuss, M. Schumacher, *J. Mol. Model.* **2006**, *12*, 591–595; c) B. E. Maki, E. V. Patterson, C. J. Cramer, K. A. Scheidt, *Org. Lett.* **2009**, *11*, 3942–3945; d) A. Kausamo, H. M. Tuononen, K. E. Krahulic, R. Roesler, *Inorg. Chem.* **2008**, *47*, 1145–1154.
[16] a) J. Bjorgo, D. R. Boyd, C. G. Watson, W. B. Jennings, D. M. Jerina, *J. Chem. Soc. Perkin Trans. 2* **1974**, *9*, 1081–1084; b) L. Jiao, Y. Liang, J. X. Xu, *J. Am. Chem. Soc.* **2006**, *128*, 6060–6069.
[17] a) A. D. Becke, *J. Chem. Phys.* **1993**, *98*, 5648–5652; b) R. H. Hertwig, W. Koch, *Chem. Phys. Lett.* **1997**, *268*, 345–351; c) P. J. Stephens, J. F. Devlin, C. F. Chabalowski, M. J. Frisch, *J. Phys. Chem.* **1994**, *98*, 11623–11627.
[18] a) V. Barone, M. J. Cossi, *Phys. Chem. A* **1998**, *102*, 1995–2001; b) M. Cossi, N. Rega, G. Scalmani, V. J. Barone, *Comput. Chem.* **2003**, *24*, 669–681; c) Y. Takano, K. N. Houk, *J. Chem. Theory Comput.* **2005**, *1*, 70–77.
[19] To conform the obtained reaction model does not depend on the treatment of noncovalent interactions of densely substituted reactants and zwitterionic intermediates; the calculations with additional diffuse function has been carried out at the CPCM-B3LYP/6-31+G(d)//B3LYP/6-31G(d) level. The calculated potential energy profiles of the most energetically favored reaction patterns for both mechanisms is very similar to that of CPCM-B3LYP/6-31G(d) level (see Supporting Information, Figure S1). The energy barrier difference between the two mechanisms is 29.6 kcal/mol, which is close to that at the CPCM-B3LYP/6-31G(d) level (30.5 kcal/mol). This indicates that the 6-31G(d) basis set is suitable for investigating the present reactions.
[20] The relative energies calculated in the gas phase are given in the Supporting Information.
[21] a) C. Gonzalez, H. B. Schlegel, *J. Phys. Chem.* **1990**, *94*, 5523–5527; b) K. Ishida, K. Morokuma, A. Kormornicki, *J. Chem. Phys.* **1977**, *66*, 2153–2156; c) C. Gonzalez, H. B. Schlegel, *J. Chem. Phys.* **1989**, *90*,2154–2161.
[22] In ref.[12a] the authors put forward the disfavored cyclization of $IN2_B$ according to Baldwin's rules to support the assumption. In fact, this step consists of a nucleophilic attack of the enolate moiety of $IN2_B$ to yield the 2-azetidinone ring and the NHC, which is a favored [4-*exo*-*tet*] reaction. For information on Baldwin's rules, see: J. E. Baldwin, L. I. Kruse, *J. Chem. Soc., Chem. Commun.* **1977**, *7*, 233–235.
[23] a) M. He, J. W. Bode, *Org. Lett.* **2005**, *7*, 3131–3134; b) D. Enders, O. Niemeier, A. Henseler, *Chem. Rev.* **2007**, *107*, 5606–5655.
[24] a) D. Enders, K. Breuer, J. Runsink, J. H. Teles, *Helv. Chim. Acta* **1996**, *79*, 1899–1902; b) J. Read de Alaniz, T. Rovis, *J. Am. Chem. Soc.* **2005**, *127*, 6284–6289; c) D. Enders, O. Niemeier, T. Balensiefer, *Angew. Chem. Int. Ed.* **2006**, *45*, 1463–1467; d) M. S. Kerr, J. Read de Alaniz, T. Rovis, *J. Org. Chem.* **2005**, *70*, 5725–5728; e) M. He, J. R. Struble, J. W. Bode, *J. Am. Chem. Soc.* **2006**, *128*, 8418–8420.
[25] a) T. Dudding, K. N. Houk, *Proc. Natl. Acad. Sci. USA* **2004**, *101*, 5770–5775; b) M. C. Kozlowski, M. Panda, *J. Org. Chem.* **2003**, *68*, 2061–2076; c) S. Bahmanyar, K. N. Houk, H. J. Martin, B. List, *J. Am. Chem. Soc.* **2003**, *125*, 2475–2479.

Received: May 30, 2010
Published Online: September 22, 2010

